

# Complex Leaching Process of Scheelite in Hydrochloric and Phosphoric Solutions

LIANG LIU,<sup>1</sup> JILAI XUE,<sup>1,5</sup> KANG LIU,<sup>1,2</sup> JUN ZHU,<sup>3</sup>  
and ZENGJIE WANG<sup>4</sup>

1.—School of Metallurgical and Ecological Engineering, University of Science and Technology Beijing, Xueyuan Road 30, Beijing 100083, People's Republic of China. 2.—Beijing Research Institute of Chemical Engineering and Metallurgy, China National Nuclear Corporation, Jiushu Road 145, Beijing 101149, People's Republic of China. 3.—State Key Laboratory of Advanced Metallurgy, University of Science and Technology Beijing, Xueyuan Road 30, Beijing 100083, People's Republic of China. 4.—College of Material Science and Engineering, Beijing University of Technology, Pingleyuan 100, Beijing 100124, People's Republic of China. 5.—e-mail: jx@ustb.edu.cn

The complex leaching process of synthetic scheelite and scheelite concentrate in hydrochloric and phosphoric solutions has been investigated for improving process efficiency. A higher leaching rate, compared with the classic acid leaching process, can be obtained through the synergy of HCl and H<sub>3</sub>PO<sub>4</sub> with appropriate W/P mole ratio, temperature, and acid concentration. For synthetic scheelite, the optimum leaching conditions were W/P mole ratio 7:1, temperature 50°C, HCl 0.72 mol/L, and stirring speed 600 rpm; for scheelite concentrate, W/P mole ratio 7:1, temperature 80°C, HCl 2.16 mol/L, and stirring speed 1000 rpm. The leaching rates under the optimized conditions can reach up to 98% or even higher. FTIR spectra analysis confirmed that the leachate composition remained as H<sub>3</sub>[PW<sub>12</sub>O<sub>40</sub>] in the range of varying W/P mole ratios, so the PO<sub>4</sub><sup>3-</sup> in acidic solution and phosphorus content in the leaching product could be better controlled. The function  $1 - (1 - X)^{1/3}$  against leaching time was applied to fit the experimental data, and the apparent activation energy,  $E_a$ , was calculated as 60.65 kJ/mol. The results would be valuable for effectively using scheelite as a raw material resource for sustainable tungsten production.

## INTRODUCTION

Tungsten is an important rare metal with a wide range of applications in modern industries and high-technologies. As the traditional mineral resources for tungsten production show a continued declining trend worldwide, several research efforts have been made to explore<sup>1-3</sup> the potential for using various scheelite ores as a raw material resource for tungsten production. The process of acid leaching scheelite demonstrates many technical and economic advantages, such as short processing flow, simple operation, and low cost. It is known that tungsten can be extracted from hydrochloric acid leaching of scheelite with a reaction constant about 10<sup>4</sup> at 293 K.<sup>4</sup> This was expected to be a fast reaction in thermodynamics, but it has preceded slowly in the leaching practice because a dense solid

layer of tungstic acid formed on the surface of scheelite particles blocking the leaching reaction.<sup>5</sup> To overcome such difficulty for improving the processing efficiency, an excess amount of acid has to be used with equipment corrosion and environmental pollution as well.

There are several studies on improving the acidic leaching process, for instance, using fine particle ore,<sup>6</sup> more excessive hydrochloric acid, and heated ball mill reactors;<sup>7,8</sup> applying hydrochloric acid with alcoholic solutions or ethylenediaminetetraacetic acid (EDTA) to digest scheelite or dissolve the solid product;<sup>9-12</sup> or leaching without the formation of tungstic acid.<sup>13</sup> These methods could eliminate, more or less, the undesired effects of a solid H<sub>2</sub>WO<sub>4</sub> layer but also could have some drawbacks, such as increased energy consumption, excess chemicals costs, and environmental pollution.

During the acidic leaching process,  $W^{6+}/Mo^{6+}$  can form water-soluble compounds with the addition of the complex reagents, such as oleic acid, citric acid, oxalic acid, tartaric acid, hydrogen peroxide, and some oxygen-containing anions like  $PO_4^{3-}$  or  $SiO_4^{2-}$ .<sup>14–17</sup> Among them,  $PO_4^{3-}$  ion is the most active chelating agent<sup>18</sup> for the complex leaching. The reaction rate in a complex acid leaching of scheelite can be accelerated by using a low-concentration acid solution (Gurmen et al.,<sup>19</sup> Rodriguez et al.,<sup>20</sup> and Zhao et al.<sup>21</sup>). Nevertheless, it is not entirely clear whether the combined effects of  $PO_4^{3-}$  containing acid solutions in cooperation with various process parameters could be brought for further improvement on the complex leaching of scheelite. In addition, a yellow solid reaction product was observed during the leaching process in  $PO_4^{3-}$  ion containing solution,<sup>18</sup> which is still not fully understood for the alternative structures of leachate generated from such complex leaching with varying  $PO_4^{3-}$  content. One possible reason for such uncertainty could be attributed to variation in the scheelite used in the leaching tests. Thus, the synthetic scheelite can be used as model material to avoid the influence of raw material variation by focusing on the nature of the leaching reaction related to the  $PO_4^{3-}$  content.

The purpose of this work is to investigate the complex leaching behaviors of synthetic scheelite and scheelite concentrate for improving process efficiency. The complex leaching rates were measured as a function of varying W/P mole ratios ( $CaWO_4/H_3PO_4$  mol ratio) and other process parameters such as temperature, acid concentration, and leaching time. The leaching rates and the corresponding composition structures of the leaching product were determined against varying W/P mole ratios. The obtained information would be valuable for effectively using scheelite ores as raw material for sustainable tungsten production.

## EXPERIMENTAL

### Materials and Chemicals

Table I shows the chemical composition of scheelite concentrate (obtained from Jiangxi province, China). Synthetic scheelite samples were prepared by using  $Na_2WO_4 \cdot 2H_2O$  ( $\geq 99.5\%$ , Sinopharm Chemical Reagent) and  $CaCl_2$  ( $\geq 96.0\%$ , Sinopharm Chemical Reagent). Stoichiometric amounts of sodium tungstate and calcium chloride were dissolved into deionized water producing solid  $CaWO_4$ :



### Leaching Process

A leaching reaction was carried out in a three-neck, flat-bottom flask and settled into a heating bath with a magnetic stirrer (DF-1, RongHua instrument manufacture). A condenser-west tube was used to hold system pressure and eliminate the water loss. The temperature of the solution was monitored by a mercury thermometer, and at the same time, it was kept on the preset value by an electronic temperature-controller (DF-1). The leaching solution was agitated with a magnetic stirrer controlled with DF-1.

The acidic solution of HCl and  $H_3PO_4$  was first diluted by adding deionized water until 100 mL and poured into the flask; the solution was then heated to the preset temperature. Afterward, 5 g of scheelite was added into the heated flask with a liquid–solid ratio of 20:1; at the same time, the timer was started. During the leaching experiment, a certain amount of solution was taken out quickly by a needle sampler with microporous membrane at a given interval for W concentration analysis. And the same amount of HCl- $H_3PO_4$  solution was fed back again to maintain constant mass of the solution. At the end of the experiment, the magnetic stirring and heating were stopped when scheelite dissolved completely or reached the preset time.

### Analysis Method

Tungsten content in the scheelite samples was analyzed quantitatively through thiocyanate method by a spectrophotometer (UV-2000, UNICO) at 405 nm and by an ICP instrument (OPTIMA 7000DV, PerkinElmer). The phases in the scheelite samples were identified using an x-ray diffractometer (Rigaku D/MAX-RB12KW). The morphology of their particles was observed by a scanning electronic microscope (JSM-6510(LA), JEOL). The structures of leaching products were inspected by Fourier transform infrared (FTIR) spectroscopy (NEXUS-670, Nicolet). The particles size distribution of the ores was analyzed by a laser granularity analyzer (LMS-30, Seishin), where anhydrous alcohol was used as dispersant by wet analysis.

## RESULTS AND DISCUSSION

### Characterization of Scheelite Raw Materials

Figure 1 is the x-ray diffraction (XRD) spectra of synthetic scheelite and scheelite concentrate before the leaching process. The comparison of their

**Table I. Chemical analysis of scheelite concentrate**

Component	$WO_3$	$SiO_2$	CaO	$Al_2O_3$	$Fe_2O_3$	$P_2O_5$	$MoO_3$	CuO	$SO_3$	$SnO_2$
Content (wt.%)	68.874	0.6797	19.041	0.1915	5.596	–	0.3129	0.3726	4.3443	0.3463

spectra indicates that the major phases for both are  $\text{CaWO}_4$ , whereas a small amount of  $\text{CaMoO}_4$  appears in the scheelite concentrate (see Fig. 1c).

Scanning electronic microscopy (SEM) images of the synthetic scheelite and the scheelite concentrate particles are presented in Fig. 2, where the former is in sphere form ranging from 2  $\mu\text{m}$  to 10  $\mu\text{m}$  in diameter, and the latter is in various irregular shapes. Particle analysis revealed that the major parts of scheelite concentrate were from 30  $\mu\text{m}$  to 80  $\mu\text{m}$  in diameter, as illustrated in Fig. 3, which were larger than those of the synthetic scheelite.

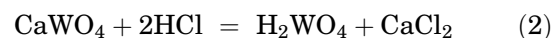
### Effect of Stirring Speed

Table II shows the leaching rate of synthetic scheelite (50°C, 0.36 mol/L HCl solutions, W/P mole ratio 7:1) with varying stirring speed. The leaching rates were determined at 5 min from the beginning of and at the end of the leaching process, which was indicated by a complete dissolution of the solid synthetic scheelite. It is obvious that the stirring intensity can affect the reaction rate to a relatively large extent at its early stage, and then, it becomes less significant at the end of the leaching process. As

a result, a stirring speed of more than 600 rpm is considered strong enough to promote the leaching reaction for the synthetic scheelite. Nevertheless, a stronger stirring of 1000 rpm for the scheelite concentrate may be required to reach the leaching rate as high as for the synthetic scheelite due to their larger and denser particles.

### Effect of W/P Mole Ratio

The chemical reaction during direct leaching scheelite in HCl solution can occur as in Eq. 2:



In the complex leaching process,  $\text{PO}_4^{3-}$  ion can act as a hetero atom with 4-coordinate (tetrahedral), and the major reaction product is hetero-poly-phosphotungstic acid with the structure of Keggin ( $\text{H}_3[\text{PW}_{12}\text{O}_{40}]$ ) or Dawson ( $\text{H}_6[\text{P}_2\text{W}_{18}\text{O}_{62}]$ ). Here the W/P mole ratio could play an important role in the complex leaching, as shown in Eqs. 3 and 4:

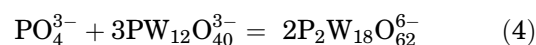
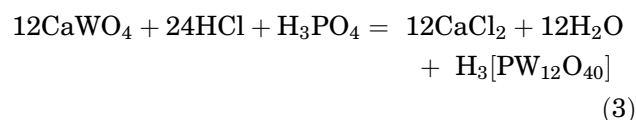


Figure 4a demonstrates an increasing trend of the leaching rate with decreasing W/P mole ratio (50°C, 0.36 mol/L HCl solution, stirring speed 600 rpm). During the later period of the leaching reaction, the function of HCl and  $\text{H}_3\text{PO}_4$  could be reduced as the effective ratio of acid to scheelite decreased due to the acid consumption in the continued leaching reaction. This could cause a delay of the leaching reaction, and the extent of such a delay could also depend on the amount of  $\text{H}_3\text{PO}_4$  addition, i.e., W/P mole ratio. For example, the time to reach the final leaching rate increased to around 5400 s for W/P = 12:1, and the others were finished between 3000 s and 3600 s with a W/P mole ratio varying from 4:1 to 10:1. Under this

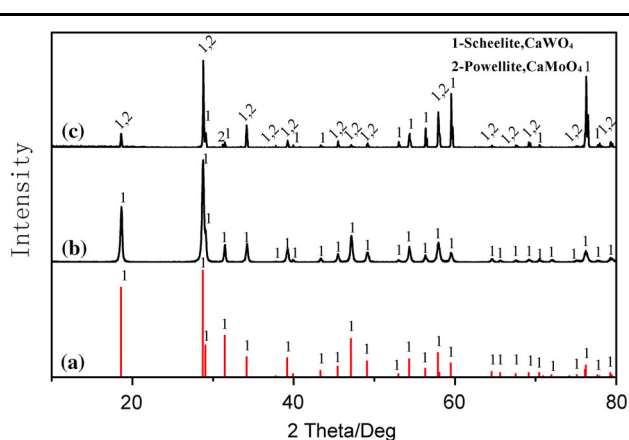


Fig. 1. XRD spectra of (a) scheelite pdf standard card (41-1431), (b) synthetic scheelite, and (c) scheelite concentrate.

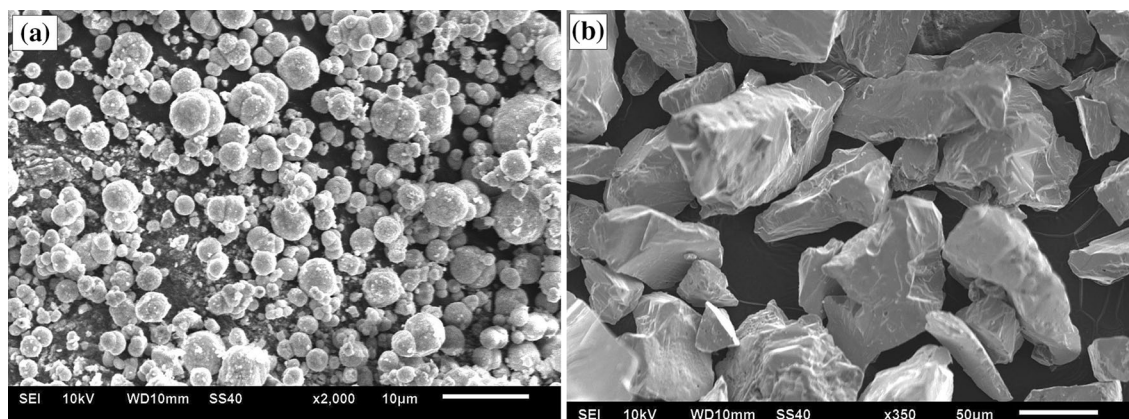


Fig. 2. SEM images of raw materials (a) synthetic scheelite and (b) scheelite concentrate.

investigation, an appropriate W/P mole ratio of 7:1 was found with the leaching rate high enough while the acid consumption remained at a moderate level, so that it was applied in all later leaching experiments.

Figure 4b shows the leaching rates with variation in the W/P mole ratio for industrial scheelite concentrate under conditions of 80°C, 2.16 mol/L HCl solution, stirring intensity 1000 rpm, leaching time 3 h. It is noted that the changing trend of the leaching rate with W/P mole ratio for scheelite concentrate is similar to the synthetic one, but the leaching rates at the same processing time are relative lower. Also the results suggest that a longer leaching time, higher temperature, and higher HCl concentration may be required in practice for leaching industrial scheelite concentrate.

### Effect of HCl Concentration

The leaching rates for synthetic scheelite, as shown in Fig. 5a, were almost the same when increasing HCl concentration up to 0.72 mol/L, 1.08 mol/L, and 1.44 mol/L (50°C, W/P mole ratio 7:1, stirring intensity 600 rpm), while the rate with HCl concentration 0.36 mol/L was found much lower than that with higher HCl concentrations.

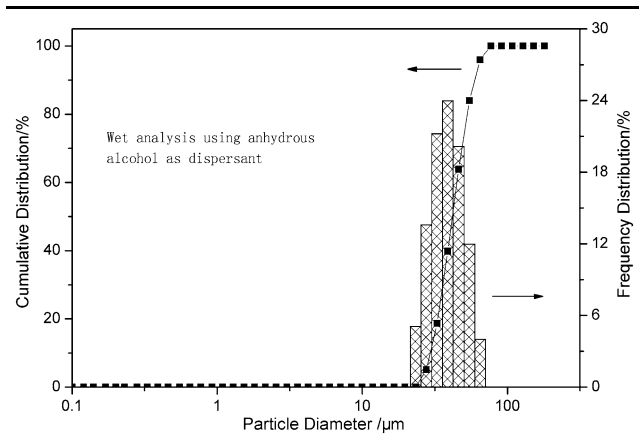


Fig. 3. Particle size distribution of scheelite concentrate.

**Table II. Leaching rate of synthetic scheelite with different stirring speeds**

Stirring speed (r/min)	Leaching rate at different time in leaching (%)	
	At 5 min from beginning	At the ending time (min)
300	37.68	95.65 (75)
400	45.80	96.23 (68)
500	43.19	96.81 (60)
600	48.41	97.39 (60)
700	63.77	95.65 (50)

Nevertheless, it seems unnecessary to test the HCl concentration higher than 0.72 mol/L in this complex leaching as the leaching rate may no longer increase along with further higher HCl concentrations.

In Fig. 5b, the leaching rates for scheelite concentrates are presented against a series of HCl concentrations (80°C, W/P mole ratio 7:1, stirring rate 1000 rpm and leaching time 3 h). When HCl concentrate was 2.16 mol/L, the leaching rate reached 98%, and a further increase in the acid concentration could give no more significant improvement in the leaching rate. For leaching the scheelite concentrate, higher HCl concentrations than the synthetic scheelite leaching have to be used. This is because not only can the gangue in the ore consume part of HCl, but also the dense particles of scheelite concentrate may need excessive hydrochloric acid to overcome the solid-liquid mass transfer resistance.

### Effect of Temperature

Figure 6a shows the temperature effects on the leaching rate in the range of 25°C to 60°C for the synthetic scheelite (0.72 mol/L HCl solution, W/P mole ratio 7:1, stirring intensity 600 rpm). The leaching rates, in general, increased with increased temperatures, and almost all could reach more than 95% at the end of the leaching reaction. This implies that the synthetic scheelite could be nearly completely dissolved within a short period when the temperature is high enough.

The variation in the leaching rate for scheelite concentrates is illustrated in Fig. 6b under the leaching condition of 2.16 mol/L HCl solution, W/P mole ratio 7:1, stirring rate 1000 rpm, and 3 h. Even with a higher HCl solution and stronger stirring intensity, the operating temperature or longer process time has to rise to reach the same leaching rates as the synthetic scheelite. For example, it could need to be at about 75°C to make the leaching rate up to 95% as those for the synthetic scheelite at the temperatures lower than 60°C. This means higher consumptions in heating energy and acid or a lower production efficiency. Moreover, the results here also suggest that any further rising operating temperature to more than 80°C may not produce significant improvement in the leaching process of the industrial scheelite concentrate.

Figure 7 demonstrates that a longer time is necessary for scheelite concentrate to have the leaching rate as high as 98% (80°C, 2.16 mol/L HCl solution, W/P mole ratio 7:1, stirring intensity 1000 rpm). In comparison with the time effect in Fig. 5a, it is suggested that a fine particle size could reduce the energy barrier to facilitate the solid-liquid mass transfer during the leaching process, so that the leaching of scheelite concentrate would be possible to have a lower temperature and shorter time.



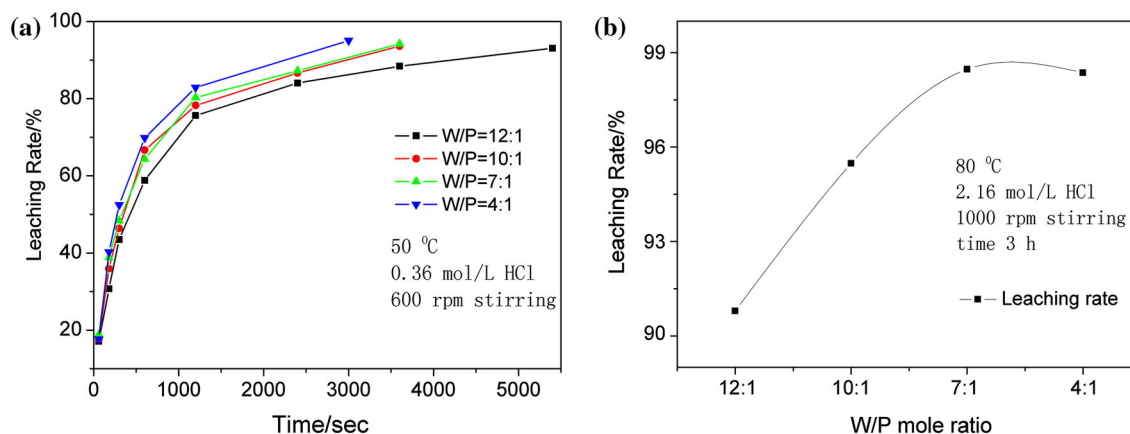


Fig. 4. Leaching rates of (a) synthetic scheelite versus time with various W/P mole ratios; (b) scheelite concentrate with changing W/P mole ratio.

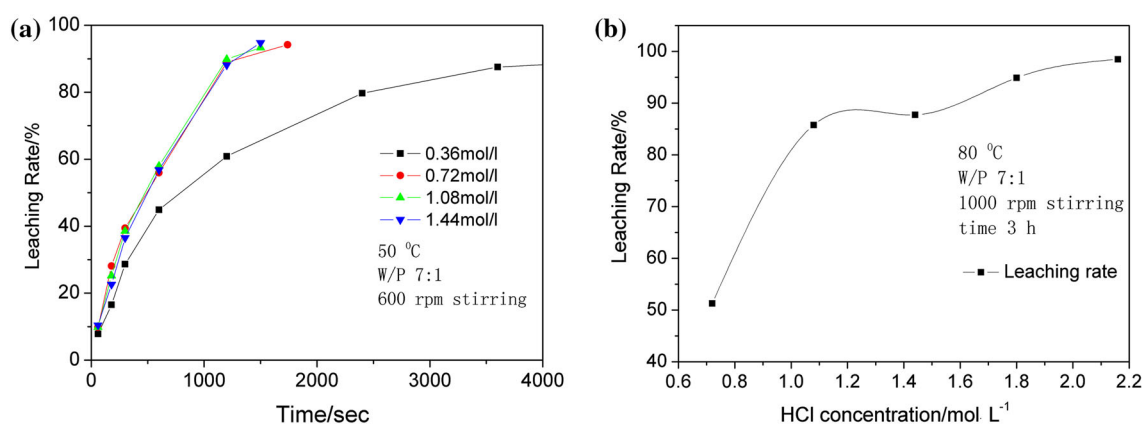


Fig. 5. Leaching rates of (a) synthetic scheelite versus time with various HCl concentrations; (b) scheelite concentrate with changing HCl concentration.

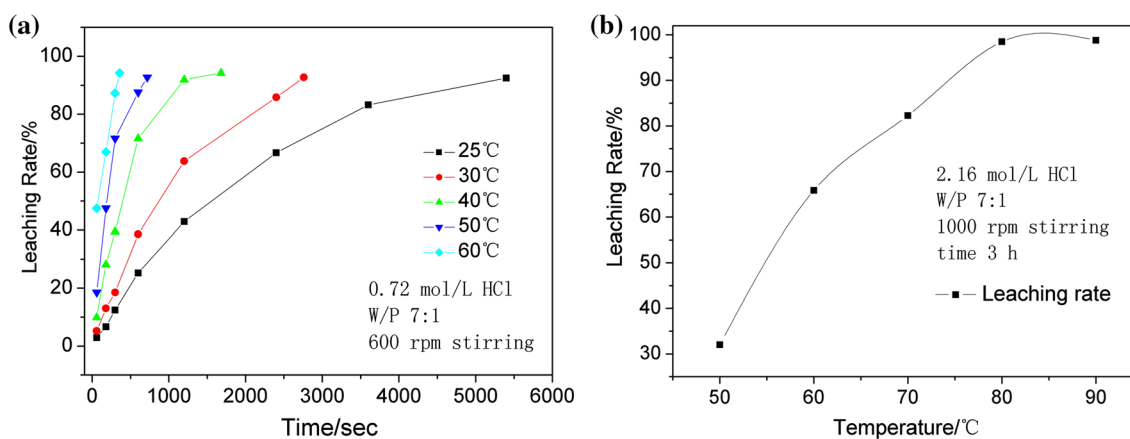


Fig. 6. Leaching rates of (a) synthetic scheelite versus time with various temperatures; (b) scheelite concentrate with changing temperature.

Table III shows the leaching efficiency of this work in comparison with others. It can be seen that complex leaching efficiency is higher than the direct acid leaching. When compared with tests 1# and 3#, the complex leaching could finish in shorter time, lower acid concentration and temperature, and higher leaching rate in treating synthetic scheelite.

When scheelite concentrate is used as raw material, 2# and 4# results show the same phenomenon even though the classic method is used in finer particle ore. This implies that the complex leaching can improve the process efficiency with lower energy and material consumption than the classic leaching method.

### Kinetic Analysis

Previous work suggested that the leaching process could be controlled by interfacial chemical reaction (Rodriguez et al.,<sup>20</sup> Zhao et al.,<sup>21</sup> Cem et al.,<sup>22</sup> and Kalpakli et al.<sup>23</sup>). In this case, the kinetics equation of the liquid–solid reaction may be written as follows:

$$1 - (1 - X)^{1/3} = k' \times t \quad (5)$$

where  $k'$  is the reaction rate constant and  $x$  is the leaching rate. In Fig. 8, the plots of the function  $1 - (1 - X)^{1/3}$  against leaching time are presented to fit the experimental data on the leaching rate.

In addition, the activation energy can be calculated from the Arrhenius equation:

$$k = Ae^{-\frac{E_a}{RT}} \quad (6)$$

where  $k$  is the reaction rate constant,  $A$  is a pre-exponential factor,  $E_a$  is apparent activation energy, and  $R$  is the molar gas constant. The Arrhenius plot for the synthetic scheelite, as shown in Fig. 9, indicates that the value of  $E_a$  is 60.65 kJ/mol. This is in good agreement with 60 kJ/mol for synthetic scheelite (Cem et al.<sup>22</sup>) and 59.9 kJ/mol for scheelite concentrate (Huang et al.<sup>24</sup>), which again suggests

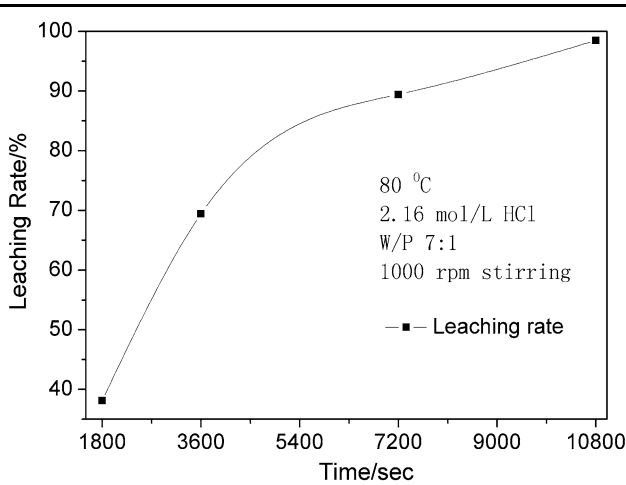


Fig. 7. Leaching rates of scheelite concentrate versus time.

that the leaching kinetic behaviors are chemically dependent on the major content,  $\text{CaWO}_4$ , in both scheelite materials.

Moreover, an empirical kinetic equation,<sup>18</sup> can be written as follows:

$$k = k_0 C_{\text{HCl}}^a C_{\text{PO}_4^{3-}}^b S^c R^d e^{-\frac{E}{RT}} \quad (7)$$

where  $k$  is the apparent reaction rate constant;  $k_0$  is the reaction rate constant;  $C_{\text{HCl}}$  and  $C_{\text{PO}_4^{3-}}$  are the initial concentrations of HCl and  $\text{H}_3\text{PO}_4$ , respectively;  $S$  is the material particle surface area; and  $R$  is the stirring speed. For this complex leaching,  $S$  and  $R$  can be incorporated into  $k_0$  to get a simplified formula, while the constants  $a$  and  $b$  can be determined by the leaching experiment. Then, the empirical kinetic equation becomes:

$$k = 6.74 \times 10^6 C_{\text{HCl}}^{1.0256} C_{\text{PO}_4^{3-}}^{0.2395} e^{-\frac{60650}{RT}} \quad (8)$$

### Effect on the Structure of the Leaching Product

There are two kinds of structures, Keggin structure or Dawson structure for hetero-poly phosphotungstic acid, which may be formed in the leaching process. Here the dosage of  $\text{PO}_4^{3-}$  decides which type of tungstate can be produced. According to Eq. 3,  $\text{H}_3[\text{PW}_{12}\text{O}_{40}]$  can be formed when the W/P mole ratio is more than 12:1. For the scheelite concentrate, it may need higher mole numbers of phosphorus as a part of  $\text{PO}_4^{3-}$  may be consumed by the gangue contents. A study<sup>18</sup> showed that when W/P mole ratio 12:1 was used, yellow tungstic acid precipitated after 20 min of reaction at  $90 \pm 0.5^\circ\text{C}$ , and this phenomenon could be due to the formation of some 2:18 tungstophosphoric acid according to Eq. 4. In this work, however, no yellow solid product has been observed for either synthetic scheelite or scheelite concentrate.

Figure 10 shows IR spectra of the leachate for the two kinds of raw materials. The infrared characteristic peaks of  $\text{H}_3[\text{PW}_{12}\text{O}_{40}] \cdot (6-7)\text{H}_2\text{O}$  (IR: KBr,  $\text{cm}^{-1}$ ) are 1080(P–O), 990(W=O), 890(W–O–W), and 810(W–O–W)<sup>25</sup>, respectively. This confirms that the leaching products for both raw materials, under different W/P mole ratios, are  $\text{H}_3[\text{PW}_{12}\text{O}_{40}]$  in the Keggin structure rather than  $\text{H}_6[\text{P}_2\text{W}_{18}\text{O}_{62}]$  in the

Table III. Leaching efficiency data of scheelite in this work (1# and 2#) and from references

No.	Raw material	Particle size ( $\mu\text{m}$ )	HCl concentration (mol/L)	Reaction temp. ( $^\circ\text{C}$ )	Reaction time (min)	Leaching rate (%)	Method
1#	Synthetic scheelite	<10	0.72	60	10	99	Complex leaching
2#	Scheelite concentrate	<80	2.16	90	180	98	Complex leaching
3# <sup>8</sup>	Synthetic scheelite	Not mentioned	4–5	70	120	90	Classic leaching
4# <sup>17</sup>	Scheelite concentrate	<44	Not mentioned	Boiling temperature	180–300	95	Classic leaching

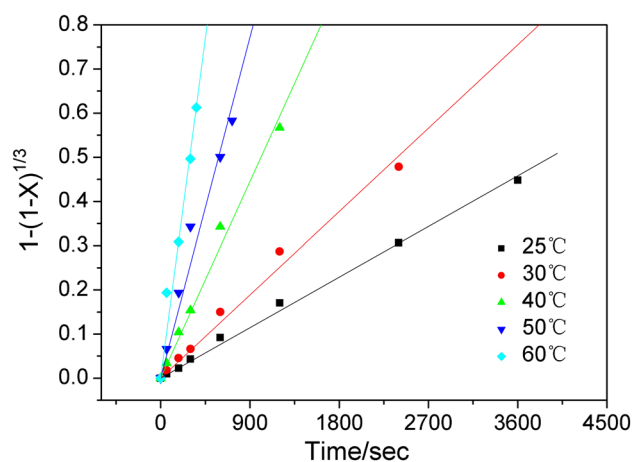


Fig. 8. Kinetics model of  $1 - (1 - X)^{1/3}$  versus time fitting the experiment data on the leaching rates of synthetic scheelite at different temperatures.

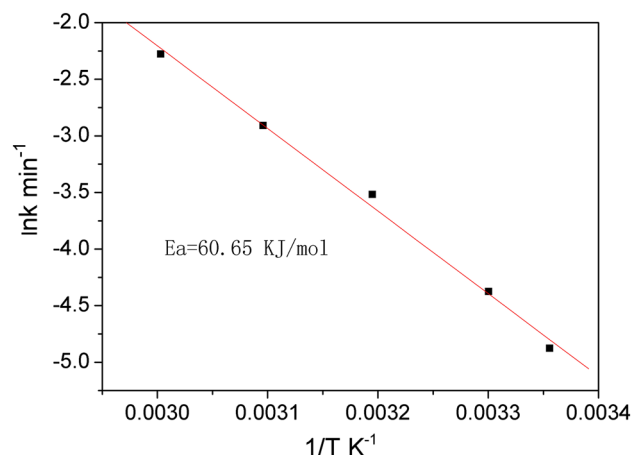


Fig. 9. Arrhenius plot for leaching reaction of synthetic scheelite at different temperatures.

Dawson structure. On the other hand,  $H_3[PW_{12}O_{40}]$  could stably exist in aqueous solutions<sup>31</sup> with the pH value  $\leq 2$ . In the leachate of synthetic scheelite, the pH value ranged from 1.18 to 1.22, while the acidity of the leachate of scheelite concentrate was even higher than the synthetic scheelite. Therefore, it is clear that the structure of leaching products is  $H_3[PW_{12}O_{40}]$  for either synthetic scheelite or scheelite concentrate, which is chemically dependent on the major content,  $CaWO_4$ , in both scheelite materials.

The yellow solid tungstic acid formed, as mentioned earlier, may not be present as  $H_6[P_2W_{18}O_{62}]$ . The superposition graph (Fig. 10b) of IR spectra shows that the huge transmittance peak at around  $3500\text{ cm}^{-1}$  is the hydroxyl characteristic peak, which has a peak intensity similar to each other with different W/P mole ratios, while the concentration of hydroxyl has the same value for three W/P mole ratios. The characteristic peaks of  $H_3[PW_{12}O_{40}]$ , however, are different, in which the weakest one is the curve with W/P mole ratio 12:1. This means that the concentration of soluble  $H_3[PW_{12}O_{40}]$  with W/P mole ratio 12:1 can be lower than that with the other two W/P mole ratios because of its lower leaching rates (ref. to Fig. 4). The significance of this result is that the formation of the Keggin structure requires less  $PO_4^{3-}$  than the Dawson structure in the leaching product, so that  $H_3[PW_{12}O_{40}]$  in the Keggin structure can completely react in the acid solution with the W/P mole ratio ranging from 12:1 to 10:1. Therefore, a higher leaching rate could be obtained by better controlling the W/P mole ratio.

After the complex leaching process, the solution was further dealt by a two-stage technology. The tungsten in the solution was first precipitated by adding ammonium chloride, and the  $(NH_4)_3[PW_{12}O_{40}]$  was obtained. Then, the precipitate was dissolved in ammonia and the impurities of Fe, P, and Mo were removed to make the purified

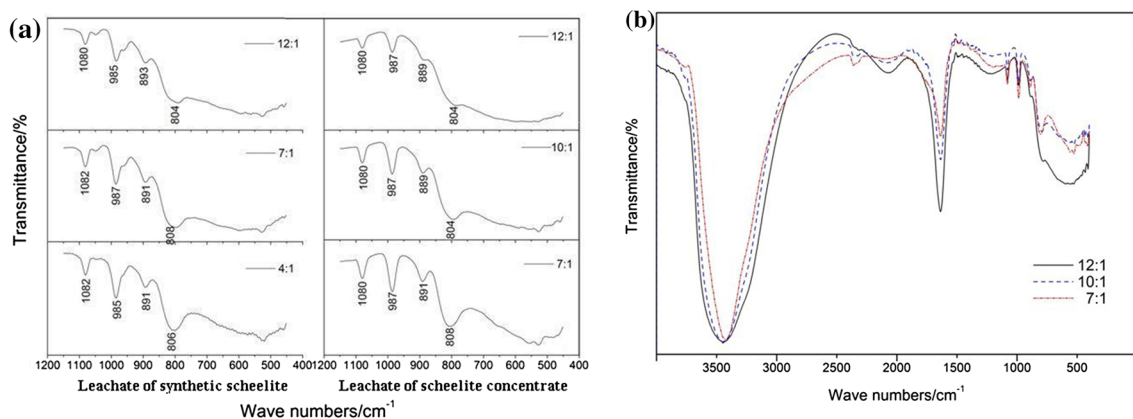


Fig. 10. IR spectra of (a) leachate of synthetic scheelite and scheelite concentrate with various W/P mole ratios; (b) superposition graph of scheelite concentrate with varying W/P mole ratio.

solution for producing APT. These later processes in purification and APT production can also be benefited by rich tungsten content in the solution obtained from the complex leaching with high efficiency.

### CONCLUSION

The complex leaching process of synthetic scheelite and scheelite concentrate in HCl and H<sub>3</sub>PO<sub>4</sub> solutions has been investigated with various processing parameters. A higher leaching rate, compared with the classic acid leaching process, can be obtained through the synergy of HCl and H<sub>3</sub>PO<sub>4</sub> with an appropriate W/P mole ratio, and such effect can be further enhanced in cooperation with optimized temperatures and acidic concentrations. For synthetic scheelite, the optimum leaching conditions were W/P mole ratio 7:1, temperature 50°C, HCl concentration 0.72 mol/L, and stirring speed 600 rpm; for scheelite concentrate, W/P mole ratio 7:1, temperature 80°C, HCl concentration 2.16 mol/L, and stirring speed 1000 rpm. The leaching rates under the optimized conditions can reach up to 98% or even higher. The function  $1 - (1 - X)^{1/3}$  against leaching time was applied to fit the experimental data, and the apparent activation energy,  $E_a$ , was calculated as 60.65 kJ/mol. FTIR spectra analysis confirmed that the leachate composition from the complex leaching process is H<sub>3</sub>[PW<sub>12</sub>O<sub>40</sub>] with varying W/P mole ratios, which could provide crucial information for better controlling PO<sub>4</sub><sup>3-</sup> in acidic solution and phosphorus content in the leaching product. The structure of such leaching products is chemically dependent on the CaWO<sub>4</sub> content in synthetic scheelite or scheelite concentrate.

### ACKNOWLEDGEMENT

The authors would like to thank financial support from the fundamental research fund for the central universities (FRF-UM-15-049).

### REFERENCES

1. Y.H. Hu and Z.H. Xu, *Int. J. Miner. Process.* 72, 87 (2003).
2. J.P. Srivastava and P.N. Pathak, *Int. J. Miner. Process.* 60, 1 (2000).
3. L. Liu and J.L. Xue, *Ceram. Trans.* 253, 157 (2015).
4. G.A. Meerson and N.N. Khavskii, *Otd. Tekh. Nauk. Metall. Topl.* 5, 36 (1961).
5. J.I. Martins, A. Moreira, and S.C. Costa, *Hydrometallurgy* 70, 131 (2003).
6. M.M. Fieberg and C.F.B. Coetzee, *Council for Mineral Technology*, Report No: M164D, 1 (1986).
7. J.A. Vezina and W.A. Gow, *Trans. Can. Inst. Min. Metall.* 69, 445 (1966).
8. A.N. Zelikman, A.S. Medvedev, and N.N. Rakova, *Tsvetnyye Metall* 4, 61 (1985).
9. I. Girgin and F. Erkal, *Hydrometallurgy* 34, 221 (1993).
10. Y. Konishi, H. Katada, and S. Asai, *Hydrometallurgy* 23, 141 (1990).
11. S. Ozdemir and I. Girgin, *Miner. Eng.* 4, 179 (1991).
12. K. Yasuhiro, K. Hiroyuki, and A. Satoru, *Metall. Trans. B* 18, 331 (1987).
13. J.I. Martins, *Ind. Eng. Chem. Res.* 42, 5031 (2003).
14. A.O. Kalpakli, S. Ilhan, C. Kahruman, and I. Yusufoglu, *Hydrometallurgy* 7, 121 (2012).
15. S. Ilhan, A.O. Kalpakli, C. Kahruman, and I. Yusufoglu, *Metall. Mater. Trans. B* 44B, 495 (2013).
16. A.O. Kalpakli, S. Ilhan, and C. Kahruman, *Eur. Metall. Conf.* 2011, 1137 (2011).
17. G.X. He, Z.W. Zhao, X.B. Wang, J.T. Li, X.Y. Chen, L.H. He, and X.H. Liu, *Hydrometallurgy* 144, 140 (2014).
18. G.H. Xuin, D.Y. Yu, and Y.F. Su, *Hydrometallurgy* 16, 27 (1986).
19. S. Gurmen, S. Timur, C. Arslan, and I. Duman, *Hydrometallurgy* 51, 227 (1999).
20. M. Rodriguez, O. Quiroga, and M.D.C. Ruiz, *Hydrometallurgy* 85, 87 (2007).
21. Z.W. Zhao, Y. Liang, and H.G. Li, *Int. J. Refract. Met. Hard Mater.* 29, 289 (2011).
22. K. Cem and Y. Ibrahim, *Hydrometallurgy* 81, 182 (2006).
23. A.O. Kalpakli and I. Yusufoglu, *Metall. Mater. Trans. B* 38, 279 (2007).
24. J. Huang, F.H. Xie, H. Xiao, and Y.M. Yang, *Chin. J. Rare Metals* 38, 703 (2014).
25. V.K. Ivan, *Catalysis by Polyoxometalates (Catalysts for Fine Chemical Synthesis)*, Vol. 2 (London: Wiley, 2002).